

Modeling and Test of a PM Synchronous Generator Based Small Stand Alone Wind Energy Converter

Eric Sambatra , Jacques Raharijaona , Georges Barakat and Brayima Dakyo
 GREAH, University of Le Havre
 25, rue Philippe LEBON 76058 Le Havre Cedex, France

Abstract—This paper deals with the study of the behavior of stand alone wind energy converters (WEC) based on permanent magnet synchronous generator (PMSG). First, the WEC chain is described and the model of each component of the conversion set is studied. At this stage, a special attention is given to incorporate the saturation effect in the PMSG model. Then, the obtained model is used to analyze the dynamic behavior of this WEC face to typical wind site profile and a variable electrical load. The obtained results help the authors to analyze the WEC performances as well as the impact of the generator saturation on the power conversion.

I. INTRODUCTION

Isolated sites electrical power supply remains a major problem of electrical engineering. They are the small scale autonomous installations lower than 10kW. Several solutions such as solar panels, petrol or diesel generator, wind generator are already used. The wind energy is used for a very long time but for environmental concern, in recent years, renewable energy production took its rise.

Recently, in wind energy industry, there has been a gradual interest to build direct coupled permanent magnet synchronous generators (PMSG) with higher power ratings. Without gearbox, a wind driven permanent magnet synchronous generator can offer some obvious advantages, such as higher overall efficiency and reliability, reduced weight [1].

The use of permanent magnets (PM) avoids external DC excitation which is necessary for magnetizing the wound rotor synchronous generator in isolated wind power plant. When the machine is assumed directly coupled, a large number of poles pairs are required to obtain reasonable values of output voltage and frequency. Consequently, a larger diameter of both rotor and stator is needed.

So, the aim of this paper is to simulate the dynamic behavior of saturated permanent magnet based stand alone wind energy converter (WEC) [2], [3]. The wind turbine is directly coupled with the PMSG. Also, the WEC is not connected on the grid. Figure 1 shows the synoptic diagram of the studied wind energy converter where one can distinguish the different components starting from the wind speed and finishing at the electrical load.

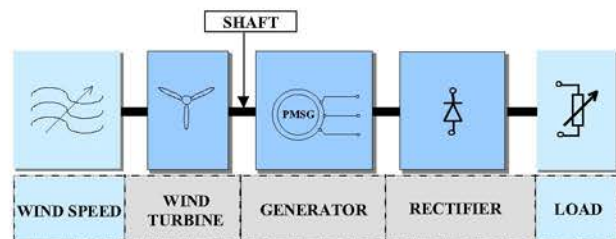


Fig. 1. Synoptic diagram of the WEC.

The WEC is located between two fluctuating (random varying) parameters which are the wind speed and the electrical load. The fluctuations of these quantities can produce several undesirable effects on the components behavior of the WEC. Indeed, in order to be able to study the dynamic behavior of these elements face to variations of fluctuating parameters, an accurate model of each element is necessary. So, the wind speed is modeled by an original approach based on Van Der Hoven spectral density [4] and the wind turbine torque is modeled thanks a polynomial approximation. Moreover, the proposed synchronous machine model in this paper includes magnetic saturation in order to predict accurately the machine performances [5]-[7].

The electrical load is then connected to the PMSG stator phases via a rectifier followed by a filter stage and an inverter [3], [8], [9]. Finally, the global model resulting from the connection of the different components models gives a powerful simulation tool helping to characterize the power conversion of this type of WEC.

II. MODELLING OF THE WEC COMPONENTS

A. Wind speed modelling based on the wind spectral characteristic of Van Der Hoven

The wind speed model is based on an original sampling of the Van Der Hoven spectral density (Fig. 2) and the expression of the wind speed is then given as follows [4]:

$$v(t) = \frac{2}{\pi} \sum_{i=0}^{N_l} A_i \cos(w_i t + \varphi_i) + \frac{2}{\pi} \sum_{i=N_l}^N A_i \cos(w_i t + \varphi_i) \quad (1)$$

where N_l and $(N-N_l)$ are the number of samples of the slow component (first term of (1)) and the turbulence component (second term of (1)) respectively, A_i and φ_i are respectively the amplitude and the phase of each

sample.

Figure 3 represents an example of the simulated fluctuating wind speed around the 9.5m/s slow component.

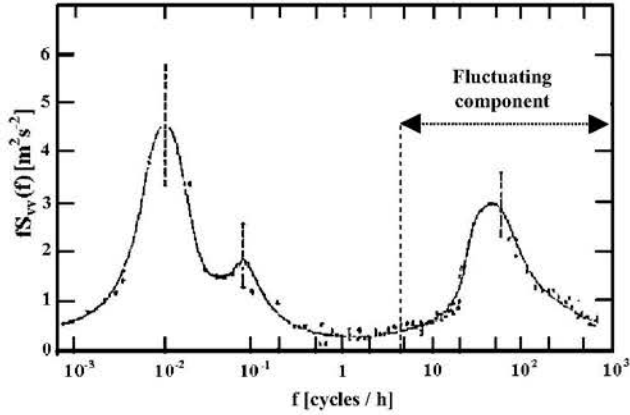


Fig. 2. Wind spectral density of Van Der Hoven.

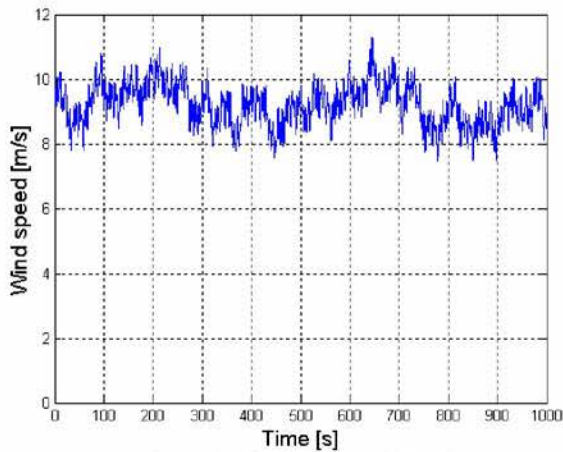


Fig. 3. Simulated wind speed (9m/s).

B. Modelling of the wind turbine torque

The wind turbine torque can be modelised by two approaches : polynomial approximation and blade pitch elements method [9].

In the case of constant blade pitch angle, the wind turbine torque is related to the wind speed by the following relation where the torque coefficient C_T is modelised by a polynomial approximation:

$$\Gamma_t(v, \Omega) = \frac{1}{2} \rho \pi R^3 v^2 C_T(\lambda) \quad (2)$$

with ρ the air density, Ω the shaft rotational speed and λ the tip speed ratio.

Figure 4 and figure 5 represent respectively the torque coefficient obtained with 6 order polynomial regression and the simulated constant wind turbine torque.

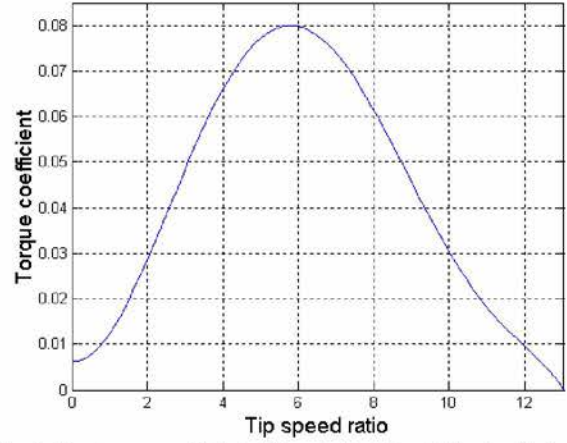


Fig. 4. The torque coefficient of the wind turbine obtained with 6 order polynomial regression.

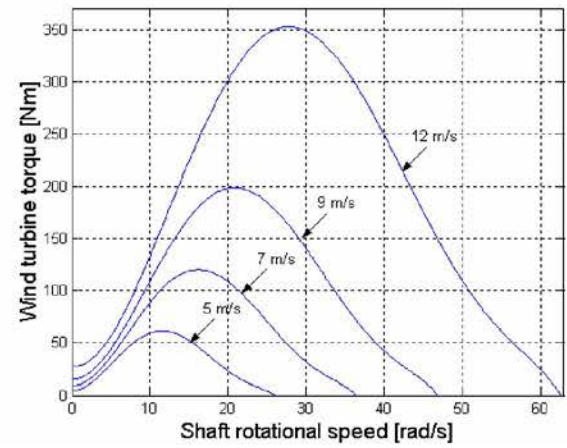


Fig. 5. Simulated constant blade pitch wind turbine torque versus the shaft rotational speed.

C. Modelling of the PMSG

The PMSG generator is modelised by considering the PM electromotive force (EMF) of the stator phase to be sinusoidal. Therefore, the stator phases voltages can be expressed as follows in a vector-matrix form [4] :

$$[v_g] = -\left\{ [r_g][i_g] + [l_g] \frac{d}{dt} [i_g] - [e_g] \right\} \quad (3)$$

$[v_g]$ is the stator voltages vector, $[i_g]$ the stator currents vector, $[e_g]$ the vector of PM EMF, $[r_g]$ the stator resistances matrix and $[l_g]$ the stator inductances matrix.

The electromagnetic torque is obtained by:

$$\Gamma_{em} = \frac{p}{2} [i_g]^T \frac{\partial}{\partial \theta} [\Phi_A] \quad (4)$$

where $[\Phi_A]$ is the vector of PM fluxes embraced by the stator phases, p is the number of pole pairs and θ the angular position of the rotor (north pole axis) with respect to the stator phase (a) axis.

To the previous equations, one must add the mechanical

equation of the generator shaft:

$$\frac{d\Omega}{dt} = \frac{1}{J}(\Gamma - \Gamma_{em} - f\Omega) \quad (5)$$

where J is the total inertia (wind turbine and generator) and f the friction.

In order to taking into account the magnetic saturation of the generator, the PMSG Park model is necessary [5]-[7]. So, applying Park's transformation, equation (3) may be rewritten in a rotor reference frame as:

$$v_d = -\left\{ R_s i_d + L_d \frac{di_d}{dt} - p\Omega L_q i_q \right\} \quad (6)$$

$$v_q = \left\{ R_s i_q + L_q \frac{di_q}{dt} + p\Omega L_d i_d - p\Omega \Phi_A \right\} \quad (7)$$

and the electromagnetic torque is expressed as:

$$\Gamma_{em} = \frac{3}{2} p [\Phi_A i_q + (L_d - L_q) i_d i_q] \quad (8)$$

v_d and i_d are respectively the d-axis voltage and current, v_q and i_q are respectively the q-axis voltage and current, R_s the stator phase resistance.

With Park transformation model, the first step is to write the magnetizing flux linkage in terms of the magnetizing current [7]. In this paper, only d-axis magnetic saturation is considered.

The relationship between the magnetizing flux linkage and magnetizing current is linear for both unsaturated and highly saturated conditions, although the slopes and intercepts of the two regions are different. The slope of this characteristic is therefore initially constant, undergoes a transition, and finally becomes constant again.

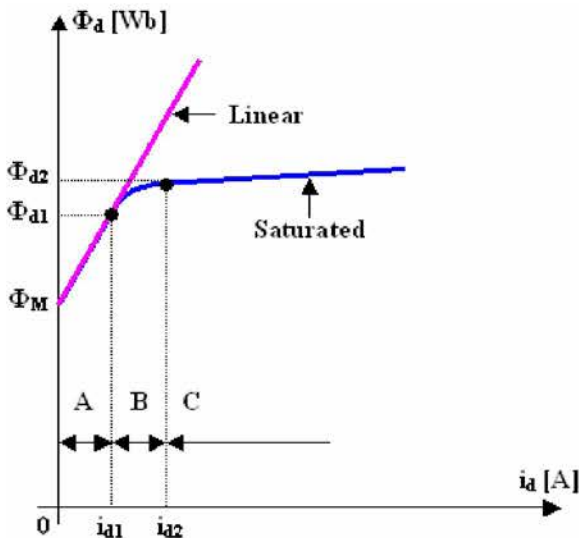


Fig. 6. Variations of the magnetizing flux linkage versus the magnetizing current of the PMSG for both linear model and saturated model.

Figure 6 represents the variations of the magnetizing flux linkage versus the magnetizing current for both linear model and saturated model.

- Region A = P_0 to P_1
- Region B = P_1 to P_2
- Region C = from P_2

where $P_0(0, 0)$, $P_1(i_{d1}, \Phi_{d1})$, $P_2(i_{d2}, \Phi_{d2})$.

A and C correspond respectively to the two linear regions of the saturated characteristic and B corresponds to the transition region.

To modelise this phenomenon, the models suggested in the literature are interpolations based on experimental measurements of the saturation characteristic of the PMSG. So, the aim of this paper is to observe the behavior of the conversion chain by considering magnetic saturation.

Thus, the authors do not establish a precise saturation model but propose a simple analytical model which reproduce the principal characteristics of this phenomenon.

The magnetic saturation characteristic is computed by the two dimensional finite element method (2D FEM). Figure 7 and figure 8 illustrate respectively the generated mesh for the PMSG finite element analysis and the flux distributions of the non loaded PMSG.

Figure 9 represents the stator phase flux versus the stator phase current obtained by the 2D FEM.

With this characteristic, the direct axis magnetizing flux linkage (Φ_d) is then expressed versus the direct axis current as follows:

$$\phi_d = \alpha_d \tanh(\beta_d L_d i_d) + \phi_M \quad (9)$$

α_d and β_d are two coefficients which can be adjusted by experimental measurements, Φ_M the PM flux linkage amplitude and L_d the direct axis inductance.

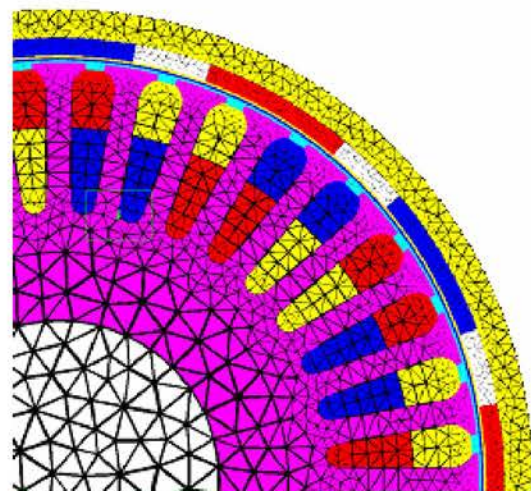


Fig. 7. Generated mesh for the PMSG finite element analysis.

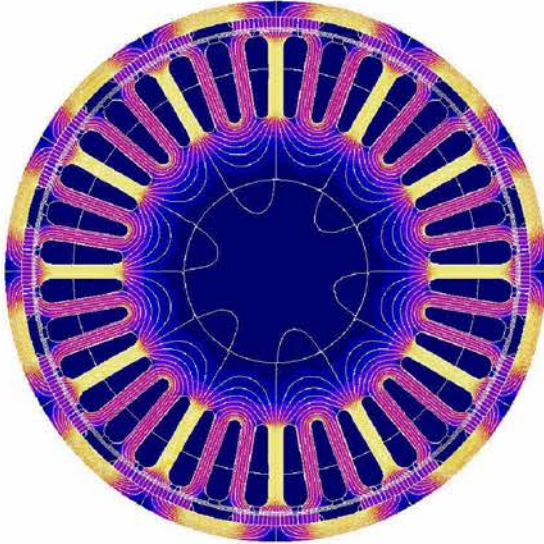


Fig. 8. Flux distributions of the non loaded PMSG.

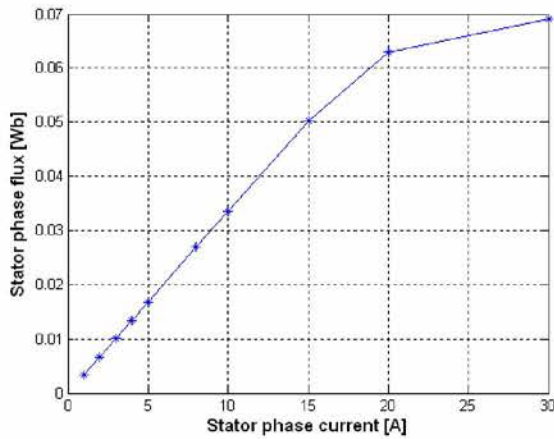


Fig. 9. Variation of the stator phase flux linkage versus the stator phase current

D. Modelling of the diode rectifier

The studied rectifier in this paper is a three-phase diode rectifier. The rectifier voltage v_R and the rectifier current i_R are connected to the phase voltages and the phase currents by means of a commutation vector [3]:

$$[S_R] = [\alpha_r \beta_r \gamma_r]^T \quad (10)$$

where the T subscript is the transpose of a vector, and α_r , β_r , and γ_r are coefficients corresponding to the stator phase voltage states.

The rectifier voltage and current are expressed as:

$$v_R = [S_R]^T [v_g] \quad (11)$$

$$i_R = \frac{1}{2} [S_R]^T [i_g] \quad (12)$$

III. DIFFERENTIAL EQUATIONS SYSTEM GOVERNING THE WIND ENERGY CONVERTER

The aim of this section is to establish the differential equations system governing the wind energy converter by connecting together the models of the different WEC components. For that, one must establish additional relationships between some state variables of the WEC model which help us to complete the differential equations system.

To establish the bond between the generator quantities and those of the electrical load, we choose to take the rectified current, the shaft rotational speed and the angular position as state variables. So, in combining the model of the PMSG with these of the diode rectifier and the electrical load, the differential equations system governing the WEC including the magnetic saturation of the PMSG is expressed as follows:

$$\begin{cases} \frac{di_R}{dt} = \frac{1}{L_{is}} \left\{ \left(R_{is} + R_{ch} \right)_R + [S_R]^T [P]^T \times \right. \\ \left. \left([e_{dqo}] + p\Omega \alpha_d \tanh([L_{ds}] [P] [S_R] i_R) \right) \right\} \\ \frac{d\Omega}{dt} = \frac{1}{J} \left\{ \Gamma_i - \left(\frac{3p}{2} [\Phi_{dqs}]^T [P] [S_R] i_R \right) - f \Omega \right\} \\ \frac{d\theta}{dt} = \Omega \end{cases}$$

where: $R_{is} = \begin{bmatrix} [S_R]^T [P] - [L_{dqs}] [P] [S_R] \\ + p\Omega [S_R]^T [P] - [L_{dqs}] \left(\frac{d[P]}{d\theta} \right) [S_R] \end{bmatrix}$

$$[\Phi_{dqs}] = \begin{bmatrix} -[L_{qs}] [P] [S_R] i_R \\ \alpha_d \tanh([L_{ds}] [P] [S_R] i_R) + \phi_M \\ 0 \end{bmatrix}$$

$$L_{qs} = [0 \ L_q \ 0]; \quad L_{ds} = [\beta_d L_d \ 0 \ 0]$$

$$L_{is} = [S_R]^T [P] - [L_{dqs}] [P] [S_R]$$

$$[R_{dqs}] = \begin{bmatrix} R_s - p\Omega L_q & 0 \\ 0 & R_s & 0 \\ 0 & 0 & 0 \end{bmatrix}; \quad [e_{dqo}] = \begin{bmatrix} 0 \\ \omega \phi_M \\ 0 \end{bmatrix}$$

$$[L_{sdq}] = \begin{bmatrix} \alpha_d \beta_d L_d \left\{ 1 - \tanh^2([L_{ds}] [P] [S_R] i_R) \right\} & 0 & 0 \\ 0 & L_q & 0 \\ 0 & 0 & 0 \end{bmatrix}$$

$[S_R]$ is the commutation vector between the PMSG and the rectifier and $[P]$ the Park transformation matrix.

IV. SIMULATION RESULTS AND DISCUSSION

By plotting the characteristics of the wind turbine torque and the electromagnetic torque of the PMSG, versus the shaft rotational speed (Fig. 9), the rectified

current versus the rectified voltage, the PMSG current versus the PMSG voltage with respect to the wind speed and the electrical load variations, several operation zones of the machine are observed.

The analysed parameters show how the mechanical quantities of the generator are affected by the dynamic properties of the wind speed of a site. It can be noticed that the variation of the load involves a significant variation of the torque at the same time the shaft rotational speed is less affected.

But in the case of wind speed changes, both torque and shaft rotational speed are more affected because C_T is significantly modified.

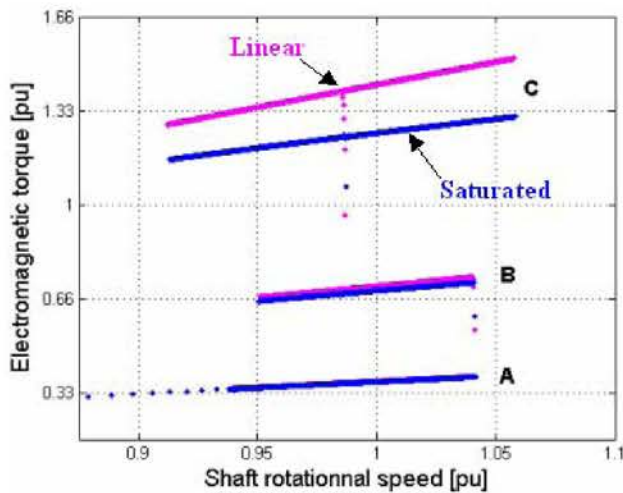


Fig. 9. The PMSG electromagnetic torque versus the PMSG shaft rotational speed for both linear model and saturated model of the PMSG

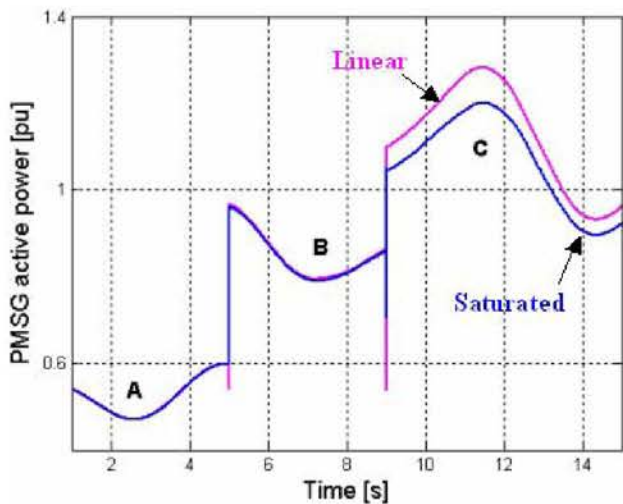


Fig. 10. The PMSG active power versus time for both linear model and saturated model of the PMSG

The representation of the output current waveform versus the output voltage gives several straight lines corresponding to the different operation regions (A, B and C) (Fig. 9 and Fig. 10).

The straight lines are due to the resistive nature of the electrical load.

The different regions A, B and C correspond to the different zones of the magnetic saturation characteristic.

A, B and C correspond respectively to the unsaturated zone, the intercept zone and the saturated zone. Figure 9 and figure 10 show that the two waveforms of both the electromagnetic torque and the PMSG active power are confused in the unsaturated zone. In the intercept zone, one can observe a light difference. This difference increases remarkably in the saturated zone.

The proposed analytical complete model is validated with experimental measurements. Figure 11 and figure 12 represent respectively the measured and the simulated rectifier current versus time corresponding to the measured wind speed profile and the resistive electrical load. One can observe a great concordance between the simulated and the measured tendencies.

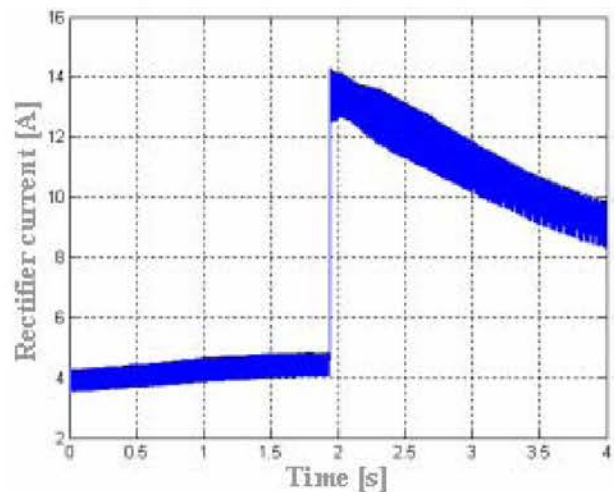


Fig. 11. Variation of the measured rectifier current versus time

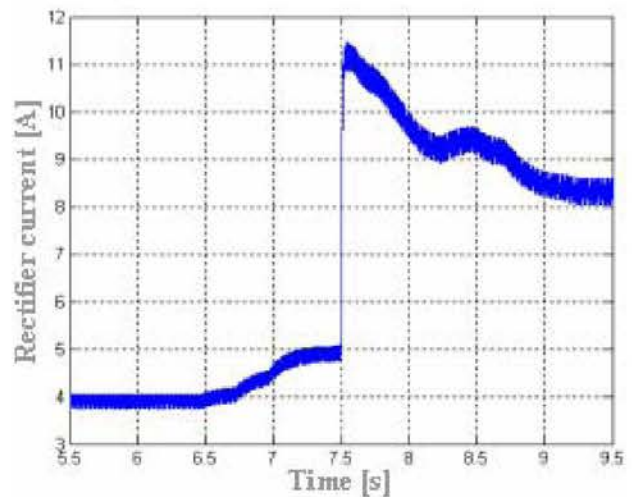


Fig. 12. Variation of the simulated rectifier current versus time

V. CONCLUSION

The behavior of a stand alone wind energy converter based on PMSG is simulated. The proposed synchronous

machine model includes magnetic saturation. The simulation results help the authors to study consequences of the wind speed fluctuations on the one hand, and variations of the electrical load on the other hand, on main quantities of the studied wind conversion chain.

Also, the magnetic saturation effect is highlighted.

The proposed analytical complete model is validated with experimental measurements. Obtained results are helpful for the design of PMSG and the control system of the WEC.

VI. APPENDIX: PARAMETERS OF THE SYSTEM

Wind turbine : BWC XL1

Rating (at $v = 11\text{m/s}$)	1 kW
Rotor radius	1.25m

Generator : Permanent magnet synchronous machine

Phase resistance	0.55 Ω
Phase inductance	5mH
PM flux linkage amplitude	0.135Wb
Number on poles	12

Shaft :

Total inertia (generator and wind turbine)	1.05kgm ²
Friction coefficient	0.001

REFERENCES

- [1] J. Y. Chen, C. V. Nayar "A multi-pole permanent magnet generator direct coupled to wind turbine", *Proceedings of ICEM'98*, vol. 3, pp. 1717 - 1722, 2 - 4 September 1998, Istanbul, Turkey.
- [2] S. A. Papathanassiou, M. P. Papadopoulos, "Dynamic behavior of variable speed wind turbines under stochastic wind", *IEEE Transactions on Energy Conversion*, vol.14, n°4, pp.1617 - 1623, December 1999.
- [3] E. J. R. Sambatra, G. Barakat, B. Dakyo "Safety operation locations of PM synchronous machine for stand alone wind energy converter", *EPE'03*, CD-ROM, 2 - 4 September 2003, Toulouse, France.
- [4] C. Nichita, D. Luca, B. Dakyo and E. Ceanga " Large band simulation of the wind speed for real time wind turbine simulator", *IEEE Transactions on Energy Conversion*, vol.17, n°4, pp.523 - 529, December 2002.
- [5] D. L. Brooks, S. M. Halpin "An improved fault analysis algorithm including detailed synchronous machine models and magnetic saturation", *Electric Power Systems Research*, n°42, pp.3 - 9, 1997.
- [6] K. Srivastava, B. Berggren "Simulation of synchronous machines in phase coordinates including magnetic saturation", *Electric Power Systems Research*, n°56, pp.177 - 183, 2000.
- [7] K. A. Corzine, B. T. Kuhn, S. D. Sudhoff, H. J. Hegner "An improved method for incorporating magnetic saturation in the q-d synchronous machine model", *IEEE Transactions on Energy Conversion*, vol.13, n°3, pp.270 - 275, September 1998.
- [8] C. L. Kana, M. Thamodharan, A. Wolf, "System management of a wind-energy converter", *IEEE Transactions on Power Electronics*, vol.16, n°3, pp.375 - 381, May 2000.
- [9] A. D. Diop, "Contribution to the development of an electromechanical wind turbine simulator Simulation and real time control of an variable blade pitch angle wind turbine," (in French), *PhD Dissertation*, GREAH, Le Havre University, France, 1999.